Transient magneto-optical spectrum of photoexcited electrons in the van der Waals ferromagnet $Cr_2Ge_2Te_6$

Erica Sutcliffe,[1] Xingjian Sun,[2] Ivan Verzhbitskiy,[2] Theodor Griepe,[3] Unai Atxitia,[4,3] Goki Eda,[2] Elton J. G. Santos,[5,6] and J. Olof Johansson[1,*]

[1]*EaStCHEM School of Chemistry, University of Edinburgh, Edinburgh EH9 3FJ, United Kingdom*
[2]*Department of Physics, National University of Singapore, 117551, Singapore*
[3]*Instituto de Ciencia de Materiales de Madrid, CSIC, Cantoblanco, 28049 Madrid, Spain*
[4]*Dahlem Center for Complex Quantum Systems and Fachbereich Physik, Freie Universität Berlin, 14195 Berlin, Germany*
[5]*Institute for Condensed Matter Physics and Complex Systems, School of Physics and Astronomy, University of Edinburgh, Edinburgh EH9 3FD, United Kingdom*
[6]*Higgs Centre for Theoretical Physics, University of Edinburgh, Edinburgh EH9 3FD, United Kingdom*

(Received 22 December 2022; revised 31 March 2023; accepted 15 May 2023; published 30 May 2023)

Femtosecond optical control of magnetic materials shows promise for future ultrafast data storage devices. To date, most studies in this area have relied on quasimonochromatic light in magneto-optical pump-probe experiments, which limited their ability to probe semiconducting and molecule-based materials with structured optical spectra. Here, we demonstrate the possibility of extracting the magneto-optical spectrum of the electrons in the conduction band in the two-dimensional van der Waals ferromagnet $Cr_2Ge_2Te_6$ (CGT), which is made possible due to broadband probing in the visible spectrum. The magneto-optical signal is a sum of contributions from electrons in the conduction and valence bands, which are of opposite sign for CGT. Depending on the probe wavelength used, this difference could lead to an erroneous interpretation that the magnetization direction is reversed after excitation, which has important consequences for understanding spin toggle switching phenomena.

DOI: 10.1103/PhysRevB.107.174432

I. INTRODUCTION

Time-resolved magneto-optical (MO) methods have been ubiquitous for the development of the field of ultrafast magnetism [1–3]. The pump-induced changes to the probe polarization state are often interpreted as a change to the magnetization of the sample [4,5]. As the research field is moving away from metals, which have a rather featureless spectral MO response in the visible region, to study novel materials such as magnetoplasmonic crystals [6,7], molecule-based magnets [8], and two-dimensional (2D) van der Waals (vdW) ferromagnets [9–20], it becomes important to explore how the spectral response of the material can affect the MO signal and how this is interpreted in terms of the magnetization dynamics.

Here, we have used time-resolved broadband MO applied to the 2D vdW semiconducting ferromagnet $Cr_2Ge_2Te_6$ (CGT) to show that the early MO dynamics (below 10 ps) is dominated by the signal from excited electrons in the conduction band for most wavelengths. We found that at certain wavelengths and pump energies, the expected demagnetization signal can be observed. The demagnetization mechanism is corroborated by simulations based on the microscopic three-temperature model (M3TM) [21–23], which indicate a fast reduction of the magnetization within 10 ps and subsequent thermal equilibration at longer times. We also observed that the excited-state and demagnetization signals have opposite signs, and that the relative contribution from the two signals changes over time, causing a sign change in the MO signal after photoexcitation. This is not an indication that the magnetization direction changes, but rather that the spectral region probes the dynamics of both the valence and the conduction band electrons. This suggests that if the entire spectral MO signal is not fully recorded, then the pure demagnetization response might be mixed with the signal from the excited electrons. In this case, the time-resolved MO signal is not necessarily a good probe of the magnetization dynamics in vdW magnets.

CGT is a layered ferromagnetic semiconductor with an indirect band gap of ∼0.7 eV [9] and is ferromagnetic below $T_c = 63$ K [24]. Since the discovery of ferromagnetism in atomic layers of CGT [25], the material has attracted substantial attention. In CGT, each Cr^{3+} ion is octahedrally coordinated to six Te^{2-} ions, with Ge^{3+} dimers spaced throughout. Ferromagnetic ordering arises in the material due to the hybridization of the Cr e_g and Te $5p$ orbitals via the nearly 90° Cr-Te-Cr bond angle [24]. The occupied Cr t_{2g} orbitals provide the bulk of the magnetic moment of the material, with the Cr e_g and Te $5p$ orbitals providing small but opposing magnetic moments [24]. Although the presence of

*olof.johansson@ed.ac.uk

magnetic anisotropy is not necessary for the stabilization of magnetism in any 2D vdW magnets [26], the balance of the crystalline and dipolar energies results in a uniaxial magnetization along the c axis of the crystal [9]. Previous calculations of the spin-projected density of states (PDOS) in CGT indicated that the Te and Ge orbitals are mostly delocalized whereas the Cr orbitals are more localized [9,27]. The band gap in the material is formed by the Te $5p$ valence band edge and the $(5p\text{-}e_g)^*$ conduction band [27,28]. The majority spin $(5p\text{-}e_g)$ and t_{2g} orbitals are well below the valence band edge, whereas their minority spin counterparts lie above the conduction band edge, emphasizing the ferromagnetic ordering in the material.

II. METHODS

In the experiments presented here, the sample consisted of a small, exfoliated crystal of CGT placed on a glass substrate and then capped with a hexagonal boron nitride (hBN) layer to protect it from oxidation. The CGT itself was grown through chemical vapor transport. A metallic mask was then applied over the sample, covering all but a 200 μm hole around the sample. The thickness of the sample (after exposure to air) was measured by atomic force microscopy [Fig. 1(b)] and was found to be 90 nm, which corresponds to several hundred layers of CGT. The ridges in the image around 15 μm are due to an imperfect calibration of the instrument.

Time-resolved optical measurements were carried out with a home-built spectrometer [29]. Unless otherwise stated, all measurements were carried out at 20 K using linearly polarized 800 nm pump pulses with a fluence of 1.0 mJ cm^{-2}. The CGT crystal was smaller than the beam waist at the laser focus, which greatly increased the noise in the experiment, as well as making it much more difficult to align accurately. This meant that it was not possible to measure static spectra, such as ellipticity, rotation, or transmittance spectra. For the transient measurements, the spatial and temporal overlap was optimized first and then the sample was moved to maximize the transient transmittance signal. The signal was very sensitive to sample position so the measurement was repeated if the sample moved (a sudden drop in signal) and the position was optimized before every experiment.

III. RESULTS AND DISCUSSION

Broadband time-resolved magnetic circular dichroism (TRMCD) spectra (which are equivalent to Faraday ellipticity spectra) were recorded for the CGT sample at $T = 20$ K after pumping at 800 nm. The lowest temperature achievable in the cryostat was chosen because we wanted to maximize the sample magnetization. The results are shown in Fig. 2(a), where the scale has been divided into a short and long range to capture the dynamics occurring on different delay times. A clear wavelength dependence can be observed at time delays shorter than ca. 10 ps. There are two short-lived positive peaks at 1.8 and 2.2 eV, overlapping with two negative peaks at 2.0 and 2.4 eV. These negative peaks are visible throughout the scan range and dominate the long-term spectral response, although a small offset of the positive peak remains at 1.77 eV.

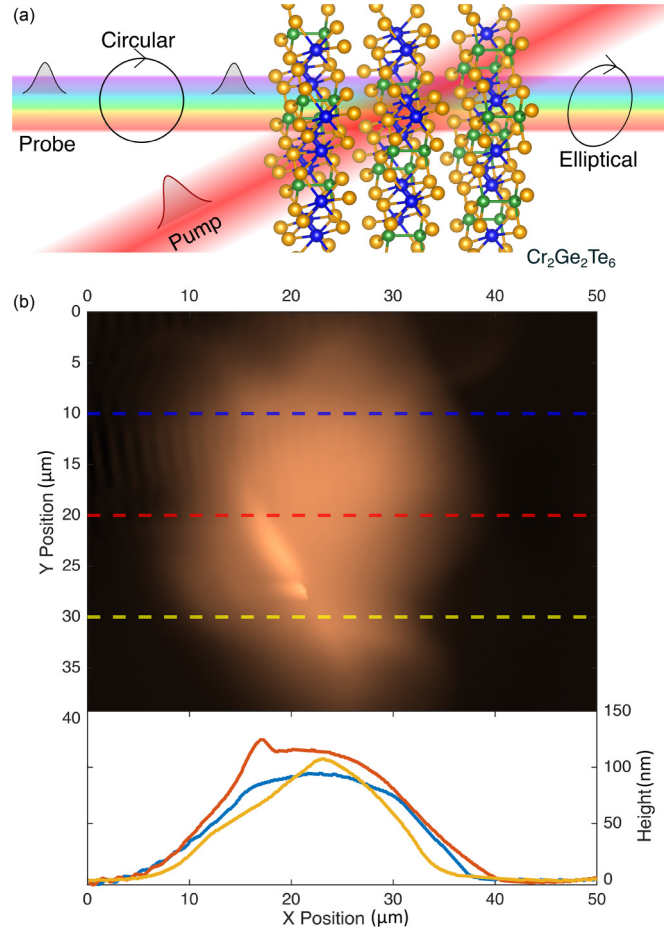

FIG. 1. Pump-probe measurements on $Cr_2Ge_2Te_6$. (a) Schematic of the application of the laser pulse experiment on the $Cr_2Ge_2Te_6$ samples which are capped with an hBN layer (not shown) to protect it against degradation. See text for details. Circularly polarized light is initially applied with the transient ellipticity measured using the method described in the text. (b) Atomic force microscopy (AFM) image of the largest crystal used in the experiment. The length profiles along the dashed lines at $Y = 10$, 20, and 30 μm are plotted directly below, showing that the thickness is approximately 90 nm. The ripples around 15 μm (red line) are a measurement artifact.

The time-resolved Faraday rotation signal from CGT, at a fixed probe energy (1.52 eV) and using a tilted external magnetic field, has previously been interpreted as a measure of the magnetization dynamics, supported by the observation of oscillations in the signal arising from ferromagnetic resonance (FMR) [30]. Furthermore, the magneto-optical Kerr effect (MOKE) signal has been used to show the complete demagnetization of CGT by performing external magnetic field sweeps at a probe energy of 1.55 eV [31]. The FMR and field sweep results are good indications that the MO signal is related to the magnetization dynamics at these probe energies.

The TRMCD signal in our data is dominated by the peak at 2.0 eV, which increases in magnitude on two timescales and reaches a plateau around 300 ps [Fig. 2(b)]. The two-step growth can be fitted to exponential functions with time constants of 1.7 and 120 ps (see details below). These timescales are comparable to those measured by Sun *et al.* for similar

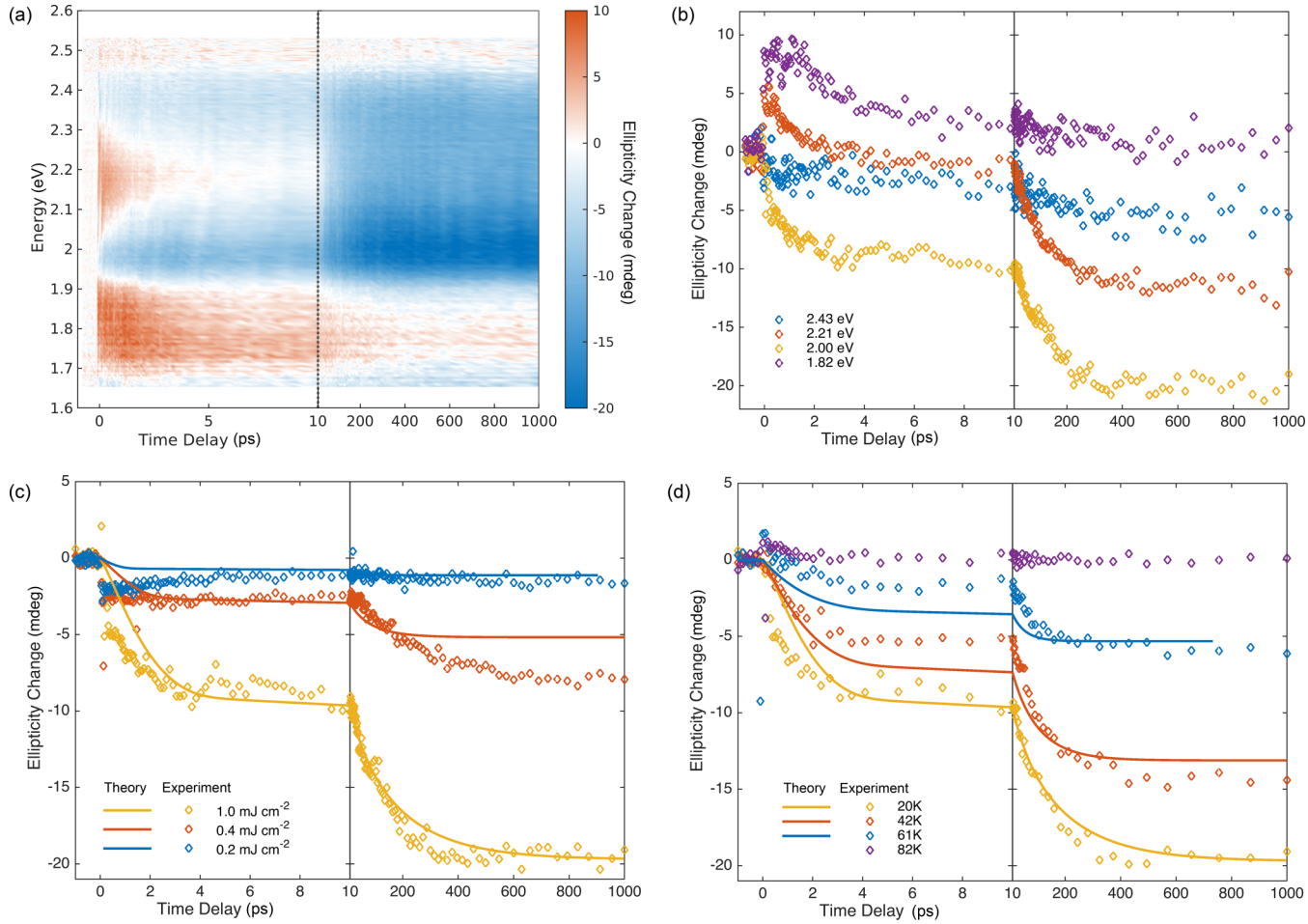

FIG. 2. Ellipticity measurements and M3TM simulations. (a) Transient ellipticity spectrum measured at 20 K using 1.55 eV, linearly polarized pump pulses (1 mJ cm^{-2}). Selected decay traces at various probe energies are plotted in (b). (c) Ellipticity change at 2.0 eV after a pump pulse of 1.55 eV at 20 K for various fluences. Dots represent the experimental data, and solid lines the M3TM simulation data. See Supplemental Material [32] for details on the modeling. (d) Change in ellipticity at 2.0 eV following a 1.55 eV pump pulse at various temperatures obtained with a fluence of 1.0 mJ cm^{-2}. Experimental and simulation data are included for comparison.

laser fluences [31], who used MOKE at 1.55 eV to demonstrate that the demagnetization occurs via a so-called type-II process [23]. In contrast to most other demagnetization studies of metals and semiconductors, Sun *et al.* found that the quenched magnetic state lived for an unusually long time, which was attributed to low thermal conductivity due to the layered nature of CGT. In agreement with Sun *et al.*, we also observed that the demagnetization is slower with lower pump fluences and lower temperatures, and that a long-lived persistent demagnetized state is formed after photoexcitation. The negative signal at 2.00 eV therefore clearly demonstrates a type-II demagnetization processes. We further validated this assignment using the M3TM [21–23], which describes the ultrafast magnetization dynamics (see Supplemental Material [32] and also Refs. [33–37] therein). The M3TM was initially applied to metallic systems [38–40], but it was soon extended to describe dynamics in semiconductors and insulators. This approach has been successful because the number of photoinduced carriers drives the system to a transient quasimetallic state. In this case, the M3TM is justified because it is possible to describe the population of electronic bands following the Fermi-Dirac distribution at an effective temperature T_e, and the thermal equilibrium of the lattice during the dynamics which follows the Bose-Einstein function with the effective temperature T_p [40]. Moreover, the M3TM approach has been successfully applied in the description of the ultrafast magnetic properties of other wide-band-gap 2D magnetic semiconductors, e.g., CrI_3 [41], which validated our approach. More details of the model are presented in the Supplemental Material [32]. To compare to the data in Figs. 2(c) and 2(d), the simulated change in magnetization was scaled to give the best fit to the measured ellipticity change. We note that the fluences used in our experiments, which are measured before the sample, are much higher than those used in the simulation. The absorbed energy by the sample will be significantly lower than the fluences reported by us because the thin sample transmits most of the pulse energy. Due to experimental constraints, it was not possible to directly measure the absorbance, however, we estimated this to be 10^{-8} J at 1.55 eV based on the measured transmittance. This value is on the same order of magnitude as in the simulations.

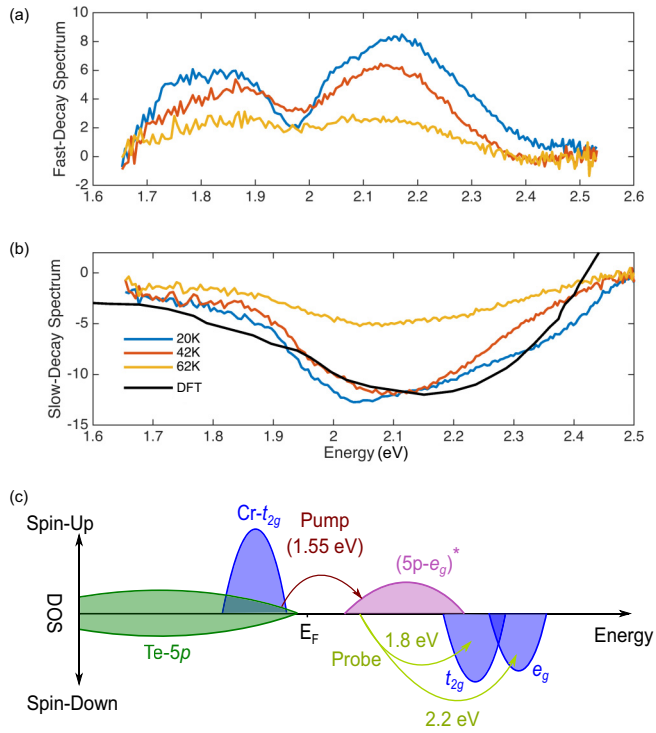

FIG. 3. Modeling of the TRMCD data. (a), (b) Extracted spectra based on the two time constants 1.7 and 120 ps, respectively, fitted from Eq. (1) to the transient ellipticity spectra at different temperatures. The fast component in (a) represents the TRMCD spectrum of the photoexcited electrons. The inverted ellipticity spectrum (shifted by 0.4 eV) calculated by Fang *et al.* [9] from density functional theory (DFT) is displayed in (b), highlighting that this component is related to the ground-state bleach signal and is a good signature of the demagnetization. (c) Schematic of the spin-projected density of states for valence and conduction states including the Fermi level (E_F). Arrows indicate the pump and probe transitions with Cr and Te states labeled.

To investigate how the shape of the spectrum changes over time, the TRMCD spectrum was fitted to a global model. We assume that the signal can be described by two independent spectra, $A_n(\lambda)$ $(n = 1, 2)$, with different time dependencies. The evolution of each spectrum is described by an exponential function with time constant τ_n, a constant offset c_n, and is convoluted with a Gaussian instrument response function of temporal width w (fixed at 0.27 ps). The constant offset terms describe a part of the signal that persists for much longer than the measured pump-probe delay (limited to the length of the translation stage). The fitted function $D(\lambda, t)$ is given by

$$D(\lambda, t) = \sum_{i=1}^{n} A_i(\lambda)\left(e^{-t/\tau_i} + c_i\right) \otimes \left(\frac{1}{w\sqrt{2\pi}} e^{-\frac{t^2}{2w^2}}\right). \quad (1)$$

This expression can be rearranged to give $A_{1,2}$ in terms of the experimentally measured $D(\lambda, t)$ [42].

Applying this model to the TRMCD data in Fig. 2 gives the fit shown in Fig. 3, with parameters $c_1 = 1.4$ and $\tau_1 = 1.7$ ps [Fig. 3(a)], and $c_2 = -2.1$ and $\tau_2 = 120$ ps [Fig. 3(b)] [32]. Given the form of Eq. (1) for $n = 2$, the resultant fit is unique. The 1.7 ps spectrum [Fig. 3(a)] has two positive peaks at 1.8 and 2.2 eV, and decays quickly to a plateau. This signal is discussed later on in the text. The 120 ps spectrum [Fig. 3(b)] has a broad negative shape that slowly grows to a long-lived state. This is the signal assigned to the demagnetization processes. It should be noted that the constant offset we find in the 120 ps spectrum is present at time zero and is attributed to the fast part of the type-II demagnetization process, which is faster than the temporal resolution of our instrument. The demagnetization signal should have the same shape as the static magnetic circular dichroism (MCD) spectrum, but scaled by an amount proportional to the change in magnetization. We observe that the 120 ps spectrum has a similar shape to the calculated ellipticity (MCD) spectrum by Fang *et al.* [9], albeit redshifted by about 0.4 eV. There is no clear temperature dependence of the time constants τ_1 and τ_2, but the offsets c_1 and c_2 decrease with increasing temperature. The amplitudes of both spectra decrease as temperature is increased, albeit in a nonlinear manner, and the shapes seem mostly independent of temperature. Type-II demagnetization was also observed in the simulations.

Pumping CGT at 1.55 eV results in a charge-transfer transition of spin-up electrons across the band gap from the nonbonding $5p$ Te orbitals into the $(5p\text{-}e_g)^*$ orbitals, which have Cr character [9,28]. The photoexcited electrons in the conduction band can be optically excited to other states that are not accessible from the valence band, such as spin-forbidden transitions that will give a different signature in the TRMCD spectrum. We assign the peaks at 1.8 and 2.2 eV to transitions from (photoexcited) Cr-centered $(5p\text{-}e_g)^*$ orbitals into spin-down t_{2g} and e_g orbitals, which would match the PDOS calculated by Kang *et al.* [27] and Fang *et al.* [9], where there are two peaks around 2 eV above the conduction band edge that are 0.4 eV apart, similar to what we observe experimentally. The t_{2g} orbital is also predicted to be broader than the e_g orbital, which agrees with the lower-energy peak in our results being broader. A schematic of the PDOS is shown in Fig. 3(c), with arrows to denote the pump and probe transitions. From the transient behavior of the positive signal, we conclude that the photoexcited carriers recombine with a 1.7 ps time constant, which is consistent with the 2 ps decay of excited carriers observed in $CrSiTe_3$ [28,32]. The temperature dependence of the TRMCD at 2.0 eV is shown in Fig. 2(d). While we do not know the Curie temperature T_c for this particular sample, it is typically around 63 K for CGT. Above 82 K, there is no observable long-term change in the ellipticity, suggesting that the there is negligible magnetic order in the system. However, on shorter timescales, a small positive signal is present that decays at a rate of around 1.8 ps is present. This signal is likely caused by the excited state ellipticity signal, which does not depend on long-range magnetic order.

IV. CONCLUSION

In conclusion, we have carried out broadband magneto-optical measurements on the layered two-dimensional ferromagnet CGT in crystalline form. We found that the Faraday ellipticity spectrum showed a rich structure with some probe energies even changing sign with time. By decomposing

the spectrum into contributions from the photoexcited and ground-state bleach signals, we could obtain the expected type-II demagnetization process and the response from the electrons in the conduction band. This method opens up possibilities for obtaining information on the spin dynamics in the excited state and highlights the need for broadband spectral probing when studying materials with rich optical properties. In this context, little is known about the spin-phonon coupling in CGT, and what type of magnetic ordering might be established when the system is away from equilibrium. For the former, recent Raman spectroscopy results [43] showed indirect electron-phonon coupling, with spin ordering acting as the intermediate between hot carriers and coherent phonons. For the latter, topological spin textures have previously been observed in CGT [44] suggesting that laser excitation might be able to induce them, as recently shown in other 2D magnets [21]. The challenge ahead therefore is to find the optimum conditions (e.g., laser fluence, temperature, substrates, high-quality samples) to manipulate and/or imprint topological spin features via laser technologies in vdW magnetic compounds.

The raw data are available online [45].

ACKNOWLEDGEMENT

This research was funded in whole, or in part, by EPSRC (EP/S018824/1 and EP/V010573/1). G.E. acknowledges support from the Ministry of Education (MOE), Singapore, under AcRF Tier 3 (MOE2018-T3-1-005) and the Singapore National Research Foundation for funding the research under medium-sized center program. U.A. gratefully acknowledges funding by the Deutsche Forschungsgemeinschaft (DFG, German Research Foundation)—Project-ID 328545488—TRR 227, Project No. A08, and Grants No. PID2021-122980OB-C55 and No. RYC-2020-030605-I funded by MCIN/AEI/10.13039/501100011033 and by "ERDF A way of making Europe" and "ESF Investing in your future." E.J.G.S. acknowledges computational resources through CIRRUS Tier-2 HPC Service (ec131 Cirrus Project) at EPCC [46] funded by the University of Edinburgh and EPSRC (EP/P020267/1), and ARCHER UK National Supercomputing Service [47] via Project d429. E.J.G.S. acknowledges the Spanish Ministry of Science's grant program "Europa-Excelencia" under Grant No. EUR2020-112238, the EPSRC Early Career Fellowship (EP/T021578/1), and the University of Edinburgh for funding support.

[1] E. Beaurepaire, J. C. Merle, A. Daunois, and J. Y. Bigot, Ultrafast Spin Dynamics in Ferromagnetic Nickel, Phys. Rev. Lett. **76**, 4250 (1996).

[2] J. Walowski and M. Münzenberg, Perspective: Ultrafast magnetism and THz spintronics, J. Appl. Phys. **120**, 140901 (2016).

[3] A. V. Kimel and M. Li, Writing magnetic memory with ultrashort light pulses, Nat. Rev. Mater. **4**, 189 (2019).

[4] B. Koopmans, M. van Kampen, J. T. Kohlhepp, and W. J. M. de Jonge, Ultrafast Magneto-Optics in Nickel: Magnetism or Optics? Phys. Rev. Lett. **85**, 844 (2000).

[5] L. Guidoni, E. Beaurepaire, and J.-Y. Bigot, Magneto-Optics in the Ultrafast Regime: Thermalization of Spin Populations in Ferromagnetic Films, Phys. Rev. Lett. **89**, 017401 (2002).

[6] S. A. Dyakov, I. M. Fradkin, N. A. Gippius, L. Klompmaker, F. Spitzer, E. Yalcin, I. A. Akimov, M. Bayer, D. A. Yavsin, S. I. Pavlov, A. B. Pevtsov, S. Y. Verbin, and S. G. Tikhodeev, Wide-band enhancement of the transverse magneto-optical Kerr effect in magnetite-based plasmonic crystals, Phys. Rev. B **100**, 214411 (2019).

[7] A. Y. Frolov, M. R. Shcherbakov, and A. A. Fedyanin, Dark mode enhancing magneto-optical Kerr effect in multilayer magnetoplasmonic crystals, Phys. Rev. B **101**, 045409 (2020).

[8] J. O. Johansson, J. W. Kim, E. Allwright, D. M. Rogers, N. Robertson, and J. Y. Bigot, Directly probing spin dynamics in a molecular magnet with femtosecond time-resolution, Chem. Sci. **7**, 7061 (2016).

[9] Y. Fang, S. Wu, Z. Z. Zhu, and G. Y. Guo, Large magneto-optical effects and magnetic anisotropy energy in two-dimensional $Cr_2Ge_2Te_6$, Phys. Rev. B **98**, 125416 (2018).

[10] M. C. De Siena, S. E. Creutz, A. Regan, P. Malinowski, Q. Jiang, K. T. Kluherz, G. Zhu, Z. Lin, J. J. De Yoreo, X. Xu, J.-H. Chu, and D. R. Gamelin, Two-dimensional van der Waals nanoplatelets with robust ferromagnetism, Nano Lett. **20**, 2100 (2020).

[11] Q. H. Wang, A. Bedoya-Pinto, M. Blei, A. H. Dismukes, A. Hamo, S. Jenkins, M. Koperski, Y. Liu, Q.-C. Sun, E. J. Telford, H. H. Kim, M. Augustin, U. Vool, J.-X. Yin, L. H. Li, A. Falin, C. R. Dean, F. Casanova, R. F. L. Evans, M. Chshiev *et al.*, The magnetic genome of two-dimensional van der Waals materials, ACS Nano **16**, 6960 (2022).

[12] D. A. Wahab, M. Augustin, S. M. Valero, W. Kuang, S. Jenkins, E. Coronado, I. V. Grigorieva, I. J. Vera-Marun, E. Navarro-Moratalla, R. F. Evans *et al.*, Quantum rescaling, domain metastability, and hybrid domain-walls in 2D CrI_3 magnets, Adv. Mater. **33**, 2004138 (2021).

[13] A. Kartsev, M. Augustin, R. F. Evans, K. S. Novoselov, and E. J. Santos, Biquadratic exchange interactions in two-dimensional magnets, npj Comput. Mater. **6**, 150 (2020).

[14] D. Abdul-Wahab, E. Iacocca, R. F. L. Evans, A. Bedoya-Pinto, S. Parkin, K. S. Novoselov, and E. J. G. Santos, Domain wall dynamics in two-dimensional van der Waals ferromagnets, Appl. Phys. Rev. **8**, 041411 (2021).

[15] F. Cantos-Prieto, A. Falin, M. Alliati, D. Qian, R. Zhang, T. Tao, M. R. Barnett, E. J. G. Santos, L. H. Li, and E. Navarro-Moratalla, Layer-dependent mechanical properties and enhanced plasticity in the van der Waals chromium trihalide magnets, Nano Lett. **21**, 3379 (2021).

[16] I. M. Alliati, R. F. L. Evans, K. S. Novoselov, and E. J. G. Santos, Relativistic domain-wall dynamics in van der Waals antiferromagnet $MnPS_3$, npj Comput. Mater. **8**, 3 (2022).

[17] M. Augustin, S. Jenkins, R. F. L. Evans, K. S. Novoselov, and E. J. G. Santos, Properties and dynamics of meron topological spin textures in the two-dimensional magnet $CrCl_3$, Nat. Commun. **12**, 185 (2021).

[18] J. Macy, D. Ratkovski, P. P. Balakrishnan, M. Strungaru, Y.-C. Chiu, A. Flessa Savvidou, A. Moon, W. Zheng, A. Weiland, G. T. McCandless, J. Y. Chan, G. S. Kumar, M. Shatruk, A. J. Grutter, J. A. Borchers, W. D. Ratcliff, E. S. Choi, E. J. G.

Santos, and L. Balicas, Magnetic field-induced non-trivial electronic topology in $Fe_{3-x}GeTe_2$, Appl. Phys. Rev. **8**, 041401 (2021).

[19] J. Meseguer-Sánchez, C. Popescu, J. García-Muñoz, H. Luetkens, G. Taniashvili, E. Navarro-Moratalla, Z. Guguchia, and E. J. G. Santos, Coexistence of structural and magnetic phases in van der Waals magnet CrI_3, Nat. Commun. **12**, 6265 (2021).

[20] L. Chen, J.-H. Chung, M. B. Stone, A. I. Kolesnikov, B. Winn, V. O. Garlea, D. L. Abernathy, B. Gao, M. Augustin, E. J. G. Santos, and P. Dai, Magnetic Field Effect on Topological Spin Excitations in CrI_3, Phys. Rev. X **11**, 031047 (2021).

[21] M. Strungaru, M. Augustin, and E. J. G. Santos, Ultrafast laser-driven topological spin textures on a 2D magnet, npj Comput. Mater. **8**, 169 (2022).

[22] M. Dąbrowski, S. Guo, M. Strungaru, P. S. Keatley, F. Withers, E. J. G. Santos, and R. J. Hicken, All-optical control of spin in a 2D van der Waals magnet, Nat. Commun. **13**, 5976 (2022).

[23] B. Koopmans, G. Malinowski, F. Dalla Longa, D. Steiauf, M. Fähnle, T. Roth, M. Cinchetti, and M. Aeschlimann, Explaining the paradoxical diversity of ultrafast laser-induced demagnetization, Nat. Mater. **9**, 259 (2010).

[24] M. D. Watson, I. Marković, F. Mazzola, A. Rajan, E. A. Morales, D. M. Burn, T. Hesjedal, G. van der Laan, S. Mukherjee, T. K. Kim, C. Bigi, I. Vobornik, M. Ciomaga Hatnean, G. Balakrishnan, and P. D. C. King, Direct observation of the energy gain underpinning ferromagnetic superexchange in the electronic structure of $CrGeTe_3$, Phys. Rev. B **101**, 205125 (2020).

[25] C. Gong, L. Li, Z. Li, H. Ji, A. Stern, Y. Xia, T. Cao, W. Bao, C. Wang, Y. Wang, Z. Q. Qiu, R. J. Cava, S. G. Louie, J. Xia, and X. Zhang, Discovery of intrinsic ferromagnetism in two-dimensional van der Waals crystals, Nature (London) **546**, 265 (2017).

[26] S. Jenkins, L. Rózsa, U. Atxitia, R. F. L. Evans, K. S. Novoselov, and E. J. G. Santos, Breaking through the Mermin-Wagner limit in 2D van der Waals magnets, Nat. Commun. **13**, 6917 (2022).

[27] S. Kang, S. Kang, and J. Yu, Effect of Coulomb interactions on the electronic and magnetic properties of two-dimensional $CrSiTe_3$ and $CrGeTe_3$ materials, J. Electron. Mater. **48**, 1441 (2019).

[28] A. Ron, S. Chaudhary, G. Zhang, H. Ning, E. Zoghlin, S. D. Wilson, R. D. Averitt, G. Refael, and D. Hsieh, Ultrafast Enhancement of Ferromagnetic Spin Exchange Induced by Ligand-to-Metal Charge Transfer, Phys. Rev. Lett. **125**, 197203 (2020).

[29] J. Sutcliffe and J. O. Johansson, A femtosecond magnetic circular dichroism spectrometer, Rev. Sci. Instrum. **92**, 113001 (2021).

[30] T. Zhang, Y. Chen, Y. Li, Z. Guo, Z. Wang, Z. Han, W. He, and J. Zhang, Laser-induced magnetization dynamics in a van der Waals ferromagnetic $Cr_2Ge_2Te_6$ nanoflake, Appl. Phys. Lett. **116**, 223103 (2020).

[31] T. Sun, C. Zhou, Z. Jiang, X. Li, K. Qiu, R. Xiao, C. Liu, Z. Ma, X. Luo, Y. Sun, and Z. Sheng, Ultra-long spin relaxation in two-dimensional ferromagnet $Cr_2Ge_2Te_6$ flake, 2D Mater. **8**, 045040 (2021).

[32] See Supplemental Material at http://link.aps.org/supplemental/10.1103/PhysRevB.107.174432 for further details regarding a comparison of the fit to the measured data, which is given in Fig. S2, where it is seen that the fit captures the main spectral and temporal features, and for fits to the transient transmittance data, which show a similar time constant and support this assignment.

[33] S. Selter, G. Bastien, A. U. B. Wolter, S. Aswartham, and B. Büchner, Magnetic anisotropy and low-field magnetic phase diagram of the quasi-two-dimensional ferromagnet $Cr_2Ge_2Te_6$, Phys. Rev. B **101**, 014440 (2020).

[34] P. Suo, W. Xia, W. Zhang, X. Zhu, J. Fu, X. Lin, Z. Jin, W. Liu, Y. Guo, and G. Ma, Terahertz emission on the surface of a van der Waals magnet $CrSiTe_3$, Laser Photonics Rev. **14**, 2000025 (2020).

[35] S. Sadasivam, M. K. Y. Chan, and P. Darancet, Theory of Thermal Relaxation of Electrons in Semiconductors, Phys. Rev. Lett. **119**, 136602 (2017).

[36] D. Zahn, F. Jakobs, Y. W. Windsor, H. Seiler, T. Vasileiadis, T. A. Butcher, Y. Qi, D. Engel, U. Atxitia, J. Vorberger, and R. Ernstorfer, Lattice dynamics and ultrafast energy flow between electrons, spins, and phonons in a 3D ferromagnet, Phys. Rev. Res. **3**, 023032 (2021).

[37] M. Beens, M. L. M. Lalieu, A. J. M. Deenen, R. A. Duine, and B. Koopmans, Comparing all-optical switching in synthetic-ferrimagnetic multilayers and alloys, Phys. Rev. B **100**, 220409(R) (2019).

[38] J. Chen, D. Tzou, and J. Beraun, A semiclassical two-temperature model for ultrafast laser heating, Int. J. Heat Mass Transfer **49**, 307 (2006).

[39] S. L. Johnson, M. Savoini, P. Beaud, G. Ingold, U. Staub, F. Carbone, L. Castiglioni, M. Hengsberger, and J. Osterwalder, Watching ultrafast responses of structure and magnetism in condensed matter with momentum-resolved probes, Struct. Dyn. **4**, 061506 (2017).

[40] F. Caruso and D. Novko, Ultrafast dynamics of electrons and phonons: From the two-temperature model to the time-dependent Boltzmann equation, Adv. Phys.: X **7**, 2095925 (2022).

[41] P. Padmanabhan, F. L. Buessen, R. Tutchton, K. W. C. Kwock, S. Gilinsky, M. C. Lee, M. A. McGuire, S. R. Singamaneni, D. A. Yarotski, A. Paramekanti, J. X. Zhu, and R. P. Prasankumar, Coherent helicity-dependent spin-phonon oscillations in the ferromagnetic van der Waals crystal Cr_3I, Nat. Commun. **13**, 4473 (2022).

[42] J. S. Beckwith, C. A. Rumble, and E. Vauthey, Data analysis in transient electronic spectroscopy – an experimentalist's view, Int. Rev. Phys. Chem. **39**, 135 (2020).

[43] J. Guo, W. Liang, and S.-N. Luo, Anomalous hot carrier decay in ferromagnetic $Cr_2Ge_2Te_6$ via spin–phonon coupling, J. Phys. Chem. Lett. **11**, 9351 (2020).

[44] M.-G. Han, J. A. Garlow, Y. Liu, H. Zhang, J. Li, D. DiMarzio, M. W. Knight, C. Petrovic, D. Jariwala, and Y. Zhu, Topological magnetic-spin textures in two-dimensional van der Waals $Cr_2Ge_2Te_6$, Nano Lett. **19**, 7859 (2019).

[45] E. Sutcliffe, X. Sun, I. Verzhbitskiy, T. Griepe, U. Atxitia, G. Eda, E. J. G. Santos, and J. Olof Johansson, "Transient magneto-optical spectrum of photoexcited electrons in the van der Waals ferromagnet $Cr_2Ge_2Te_6$", doi: 10.7488/ds/3793 (2023).

[46] http://www.cirrus.ac.uk.

[47] http://www.archer.ac.uk.